Available online at www.sciencedirect.com
ScienceDirect
Journal of Photochemistry and Photobiology A: Chemistry 194 (2008) 143–147
Journal of Photochemistry and Photobiology A:Chemistry
www.elsevier.com/locate/jphotochem

Photoelectrochemical characteristics of cells with dyed and undyed nanoporous p-type semiconductor CuO electrodes

Seiichi Sumikura, Shogo Mori, Sinya Shimizu, Hisanao Usami, Eiji Suzuki *

Department of Fine Materials Engineering, Faculty of Textile Science and Technology, Shinshu University, 3-15-1 Tokida, Ueda, Nagano 386-8567, Japan

Received 24 November 2006; received in revised form 12 July 2007; accepted 31 July 2007
Available online 6 August 2007

Abstract

We prepared nanoporous p-type CuO semiconductor electrodes adsorbing various dyes with different HOMO levels and anchoring groups. Solar cells were fabricated by coupling each of the dyed electrodes with a platinum counter electrode and filled with electrolytes containing I^-/I_3^- redox couple. Cathodic photocurrent due to hole injection from the adsorbed dye to the semiconductor was observed. Only the dyes with HOMO and LUMO potentials more positive than valence and conduction band edges, respectively, functioned as sensitizers for p-type dye-sensitized solar cells. Effects of annealing temperature and thickness of the CuO nanoporous membrane on cell performance were investigated as well.

Keywords: Hole injection; Potential difference; Energy conversion efficiency; Cathodic current

1. Introduction

Since a dye-sensitized solar cell (DSC) with 7% solar to power conversion efficiency was reported by O'Regan and Grätzel in 1991 [1], DSCs have attracted attention due to their high efficiency and expected low production cost. To date, the highest reported efficiency, which is above 11%, was achieved by a nanoporous TiO_2 electrode sensitized with a Ru complex dye absorbing light between 400 and 800 nm of solar spectrum [2]. In order to increase the efficiency further, wider light spectrum should be harvested. However, it is not trivial to design single dye absorbing wide range of the spectrum. In addition, to exploit lower energy photons of near IR region, open circuit voltage (V_{OC}) of the solar cells must be decreased. A remedy of the issues is to introduce tandem structure to DSCs.

In 2000, He et al. reported a tandem solar cell using dye-sensitized TiO_2 as a photo-anode and dye-sensitized NiO, a p-type semiconductor, as a photo-cathode for longer wavelength spectrum [3]. Dye sensitization of the photo-cathode occurs due to hole injection from the adsorbed dye to the NiO. The photo-anode and -cathode were connected in series through an electrolyte containing I^-/I_3^- redox couple. For the case, V_{OC} becomes the potential difference between the Fermi levels of the TiO_2 and NiO. In principle, the same values of J_{SC} can be obtained from the anode and cathode by using dyes absorbing equal number of photons, and thus, a higher efficiency can be expected for the tandem DSCs than conventional one.

At the moment, efficiency of dye-sensitized p-type metal oxide semiconductor is very low, which limits the efficiency of the tandem cell using dye-sensitized n- and p-type metal oxide electrodes (n/p DSCs). The highest reported values for dye-sensitized p-type metal oxide solar cells (p-DSC) using NiO were 1 mA cm^{-2} of J_{SC} and 80 mV of V_{OC} [4,5]. The reasons of low efficiency have not been understood yet, and knowledge of p-type semiconductors as hosts of dye-sensitization is limited. In order to expand knowledge and understanding of p-type dye-sensitization for solar cells, we studied photocurrent characteristics of CuO nanoporous electrodes instead of NiO electrodes used by He et al. as photo-cathodes adsorbing various dyes with the different highest occupied molecular orbital (HOMO) and lowest unoccupied molecular orbital (LUMO) levels, comparing with that of undyed CuO nanoporous electrodes.

A widely recognized concept how p-type dye-sensitized cells function is the following: the hole injection is electron transfer from the valence band of the semiconductor to the vacant HOMO

* Corresponding author. Tel.: +81 268 21 5456; fax: +81 268 21 5456.
E-mail address: esuzuki@shinshu-u.ac.jp (E. Suzuki).

1010-6030/$ – see front matter © 2007 Elsevier B.V. All rights reserved.
doi:10.1016/j.jphotochem.2007.07.035

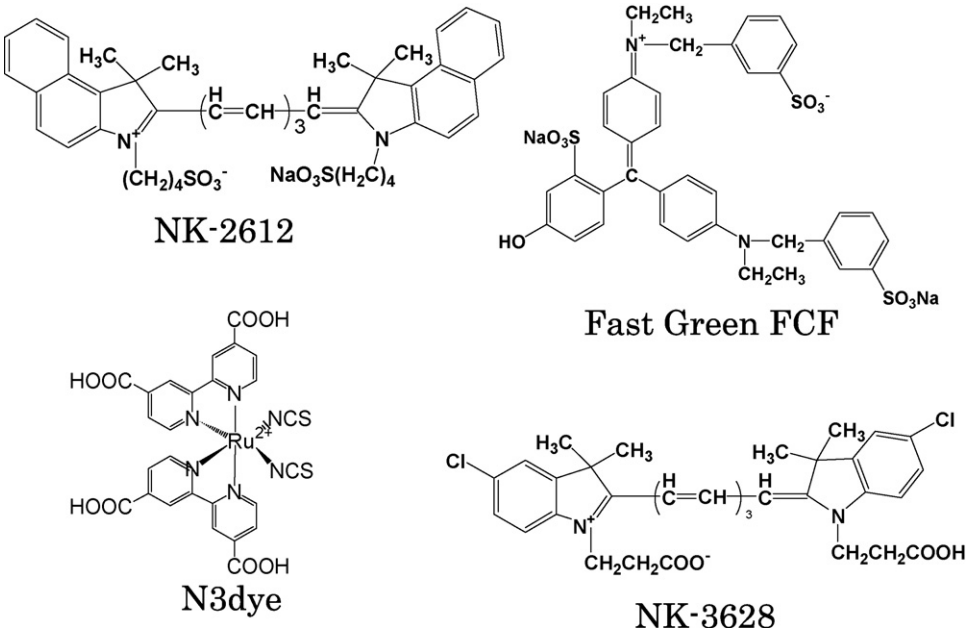

Fig. 1. Structure of examined dyes.

of the photoexcited dye [6]. The injected holes diffuse to the back contact, and electrons photoexcited from the HOMO to the LUMO transfers to I_3^- in the electrolyte, yielding cathodic photocurrent [4]. Discussion in this study is mainly based on this concept.[1]

CuO is a p-type semiconductor whose bandgap is 1.4 eV [7]. The dyes examined here have the potential difference between the HOMO and LUMO larger than 1.4 eV. Therefore, they are not suitable for expanding photoactive spectrum of CuO electrode to a longer wavelength range. The dyes, however, are expected to enhance photocurrent in the range of CuO absorbing spectrum, and the primary aim of the study here is to investigate conditions giving the hole injection at electrolyte/dye/CuO interfaces. Along the purpose, we selected dyes having various HOMO levels relative to the valence band edge potential of CuO and different anchoring groups.

2. Experimental

Porous CuO film was prepared by applying CuO slurry (C.I. KASEI Co., Ltd.) on FTO (9.5 Ω/square; Nippon Sheet Glass Co., Ltd.) by doctor blade method using mending tape (Scotch®) as a spacer. The film was annealed at 300, 400 or 500 °C for 30 min. The film was characterized by XRD measurements (Rigaku RINT system, Cu Kα) and field emission-scanning electron microscopy (FE-SEM; HITACHI S-5000). Thickness of the films was measured with a surface profiler (KLA-Tencor Co. Ltd., Alpha-step 500).

For sensitization, we examined four dyes; NK-2612, NK-3628 (Hayashibara Biochemicals Laboratories, Inc.), Fast Green FCF (Wako Pure Chemical Industries, Ltd.), and N3 (Peccell Technologies, Inc.). Fig. 1 shows structure of these dyes. Absorption peak (λ_{max}), the highest occupied molecular orbital (HOMO) and the lowest unoccupied molecular orbital (LUMO) potentials of the dyes were determined as follows. Oxidation potentials of ground state dyes were measured by cyclic voltammetry (CV) or differential pulse voltammetry (DPV) using an electrochemical analyzer (model 650A, ALS instruments), and used as the HOMO potentials in our study. Reference electrode was Ag/AgCl, and working and counter electrodes were Pt wires. The optical absorption spectra in the range 400–900 nm were recorded with spectrophotometer (U-4100; HITACHI, Ltd.). Fluorescence spectrum measurement (F-4500; HITACHI, Ltd.) was carried out for the solutions containing 0.1–0.01 mM of the dyes in a quartz cell. They were bubbled with argon or nitrogen gas for 5 min before measurements. Stray light was cut with a bandpass filter. The energy gap of dyes (E_g) was calculated from Eq. (1) with long wavelength of absorption edge (λ_1) or short wavelength of fluorescence edge (λ_2). λ_1 was used when fluorescence was not observed.

$$E_g = h\nu_{1\,or\,2}(J) = \frac{1240}{\lambda_{1\,or\,2}(\mathrm{eV})}, \quad (1)$$

where h is the Planck constant, ν frequency, and λ the wavelength of the absorption or fluorescence edge.

LUMO potential was calculated by using Eq. (2).[2]

$$\mathrm{LUMO} = \mathrm{HOMO} - E_g \quad (2)$$

[1] There may be surface states or other states in band gap into which the holes or electrons may be injected. Therefore comparing the HOMO and LUMO levels with the Fermi level may be more strict method. However, the authors follow for the time being the widely applied simplified model that the holes are injected from the HOMO to the valence band in p-type cells and the electrons are injected from the LUMO to the conduction band in n-type cells [4,6]. Therefore, the authors compare the HOMO and LUMO levels with the valence and conduction band edges.

[2] LUMO potential estimated by Eq. (2) is not based on one electron approximation, but includes the electron correlation.

DSCs were fabricated by coupling the dye-adsorbed films with Pt/Pd sputtered FTO as a counter electrode, and by filling between the two electrodes an electrolyte containing 0.05 M I_2, 0.1 M LiI, 0.6 M 1,2-dimethyl-3-propylimidazolium iodide (DMPII), and 0.5 M 4-*tert*-butylpyridine in acetonitrile. *I–V* characteristics were measured using solar simulator (AM1.5 100 mW cm^{-2}, YSS-100, Yamashita Denso Co. Ltd.) and a cyclic voltammetry tool (HSV-100; Hokuto Denko Co., Ltd.). For incident photon to current conversion efficiency (IPCE) measurement, DSCs were irradiated with monochromatic light and short circuit current was measured with a digital multimeter. IPCE was obtained by Eq. (3).

$$\mathrm{IPCE}(\%) = 1240\left(\frac{J_{SC}}{\lambda\phi}\right)100, \tag{3}$$

where J_{SC} is short circuit current density (mA cm^{-2}), λ wavelength of monochromatic light (nm), and ϕ intensity of monochromatic light (mW cm^{-2}).

3. Result and discussion

3.1. XRD measurements

Fig. 2 shows XRD pattern of CuO film annealed at 300 °C. All peaks were assigned to those of CuO but not of Cu_2O by comparing the peak position with JCPDS card nos. 50611 and 50667. Crystal size was estimated by using Scherrer equation:

$$D = \frac{K\lambda}{b\cos\theta} \tag{4}$$

where D is primary particle size, K constant, 0.9 in this case, λ X-ray wavelength (0.15421 nm; Cu Kα), b half width (rad), and θ the reflection angle. The estimated particle size was 16 nm.

3.2. Dye-sensitization

Electrochemical and light-absorbing characteristics of the dyes determined in this study were summarized in Table 1.

Photoelectrochemical characteristics of the cells fabricated using the dye-adsorbed and non-adsorbed CuO electrodes are measured using the solar simulator. Fig. 3 shows *I–V* characteristics of the cells. The cells exhibited the highest J_{SC} with Fast Green FCF and the highest V_{OC} with NK-3628 when irradiated. The photon-to-current conversion efficiency of the cells was enhanced 5.3- and 3.6-fold by dying with Fast Green FCF and with NK-3628 dyes, respectively, in comparison with the undyed CuO cell. On the other hand, N3 dye reduced the cell efficiency to 1/20 of the undyed CuO cell. To further examine characteristics of the increase or decrease in the efficiency with dyeing, incident photon to current efficiency (IPCE) at each wavelength was measured (Fig. 4). IPCE peaked at around 620 and 790 nm for Fast Green FCF and NK-3628, respectively. The peak wavelength is close to the absorption maximum wavelength

Table 1
HOMO and LUMO potential of dyes and peak wavelength of absorption

Dye	λ_{max} (nm)	HOMO[a] (V)	LUMO[a] (V)
Fast Green	615	1.25	−0.74
NK-2612	786	0.60	−0.88
NK-3628	752	0.90	−0.75
N3	525	1.00	−0.97

[a] vs. NHE.

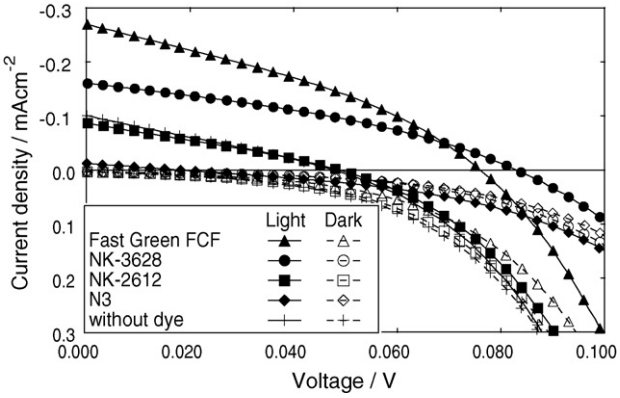

Fig. 3. *I–V* characteristics of p-DSCs using CuO electrodes dyed with four different dyes and an undyed CuO electrode. Irradiation intensity was 100 mW cm^{-2}.

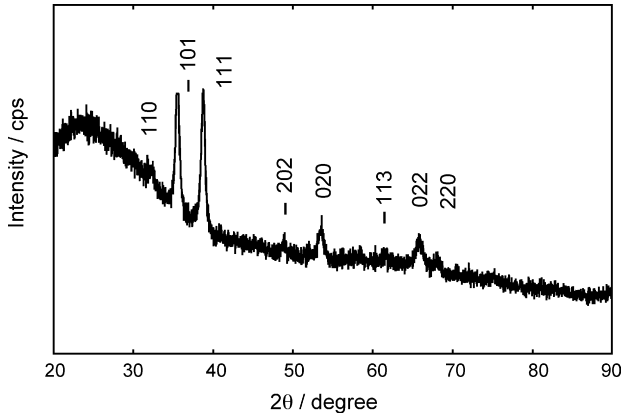

Fig. 2. XRD pattern of CuO film annealed at 300 °C.

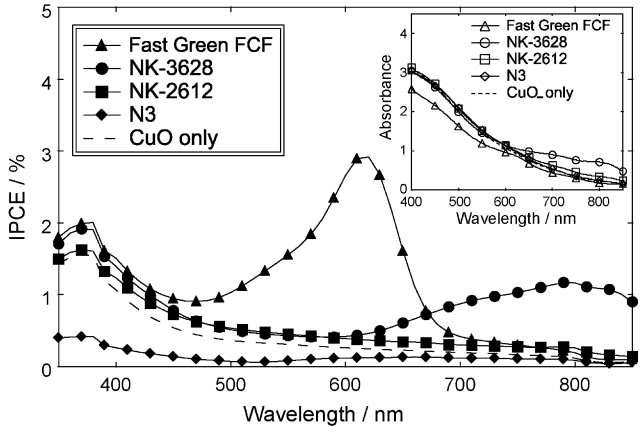

Fig. 4. IPCE of p-DSCs using CuO electrodes dyed with four different dyes and an undyed CuO electrode. Inset: Absorption spectra of each dyed and undyed nanoporous CuO electrode. CuO film thickness is 0.34, 0.41, 0.52, 0.42 and 0.36 μm for Fast Green FCF dye, NK-3628, NK-2612, N3 and without dye.

(λ_{max}) of Fast Green FCF, 615 nm and of NK-3628, 752 nm, respectively. These results indicated the CuO electrodes were dye-sensitized by Fast Green FCF and NK-3628. Since the current was enhanced to cathodic direction, the authors concluded that hole injection caused the dye-sensitization. NK-2612 dye did not show any IPCE peak in the wavelength range corresponding to the dye absorption. N3 dye showed IPCE valley instead of peak in the wavelength range corresponding to the dye absorption, indicating that dying with N3 depressed photocurrent generated by direct excitation of CuO, in other words, N3 dye exhibited negative dye-sensitization for p-type CuO electrode. In some cases, CuO electrode dyed with N3 generated anodic current (data not shown) instead of cathodic one.

The inset of Fig. 4 shows absorption spectra of the dyed and undyed CuO electrodes. Although the CuO electrodes were thin, CuO itself absorbed most of visible light. Absorption due to the adsorbed dye was seen only for NK-3628. However, the cell with undyed CuO did show much lower performance than the cells dyed with Fast Green FCF and NK-3628 as shown in Fig. 3. The fact suggested that electrons and holes generated by direct excitation of semiconductor CuO tend to quickly recombine, resulting in the low cell efficiency, while with dye-sensitization only the holes are injected to CuO and the excited electrons in the dye molecules are transferred to I_3^- in redox solution, resulting in better charge separation and consequently the higher cell efficiency. Defect sites in nanoporous CuO film can be recombination sites; CuO used in this study are far from defectless crystals and expected to have many defect sites.

3.3. CuO band edge potentials relative to HOMO and LUMO

The valence band edge was estimated as sum of the open circuit voltage (V_{OC}) and I^-/I_3^- redox potential. The value of *V*oc is the difference between the redox potential of the electrolyte and the Fermi level of p-type semiconductor. Here, we assume the Fermi level is located close to the valence band edge. Observed V_{OC} of 0.08 V, and the I^-/I_3^- redox potential of 0.44 V vs. NHE [8] yielded the valence band edge potential E_{VB} of 0.52 V vs. NHE. The conduction band edge potential E_{CB} of CuO was estimated as −0.8 V vs. NHE by subtracting the band gap energy from the valence band edge potential.

Potentials of the valence and conduction band edges of CuO and the HOMO and LUMO of the dyes are shown in Fig. 5. HOMO levels of Fast Green FCF, N3 and NK-3628 seem to be deep enough to inject holes into the valence band. Among them, the potential difference between the Fast Green FCF HOMO and E_{VB} is largest, seeming to give the fastest hole injection rate and resulting in the highest cell performance.

The HOMO level of NK-2612 does not seem to be sufficiently deeper than E_{VB} to inject holes to the valence band, which is consistent with no dye-sensitization observed for this dye.

The LUMO level of N3 is sufficiently above E_{CB} to inject the photoexcited electrons from the dye to the conduction band; the injected electrons would recombine in CuO with the holes generated by direct excitation of CuO or injected from N3 dye, which explains the observed negative dye-sensitization and anodic current exhibited in some cases by N3 dye. Since the HOMO level of N3 is sufficiently deeper than E_{VB}, there may be considerable hole injection. However, since the LUMO is distributed closer to the semiconductor than the HOMO in adsorbed N3 [9], the electron injection from the dye to CuO possibly overwhelms the hole injection.

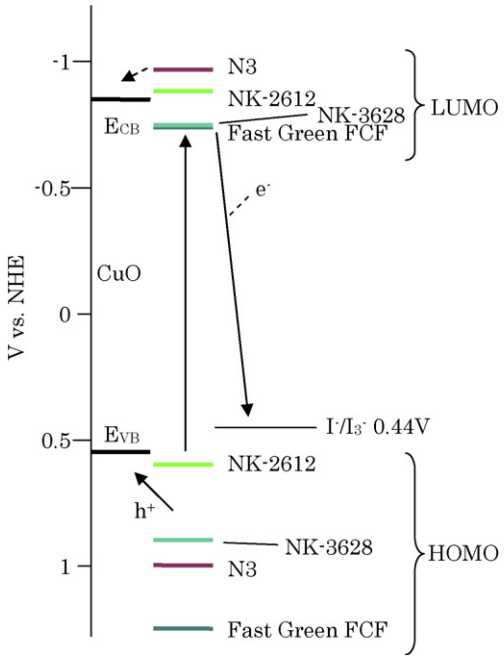

Fig. 5. Energy diagram of the dyes and CuO.

The LUMO levels of Fast Green FCF and NK-3628 are below E_{CB} and consequently no electron injection seems to occur, resulting in less recombination of the electrons and holes in CuO.

3.4. Calcination temperature of CuO electrode

Fig. 6 shows FE-SEM images of CuO electrodes annealed at 300, 400 or 500 °C. As the temperature increased, larger particles were formed, probably due to melting of boundaries between particles. Table 2 shows *I–V* characteristic of the cells dyed with Fast Green FCF. The cells showed lower J_{SC} with CuO electrode annealed at 500 °C than at 300 and 400 °C, which could be due to the smaller dye adsorbing surface area of the larger particles formed at 500 °C.

Table 2
I–V characteristics of p-DSCs prepared with different CuO annealing temperatures

Temperature (°C)	J_{SC} (mA cm^{-2})	V_{OC} (V)	Fill factor	η (%)
300	0.30	0.115	0.31	0.011
400	0.36	0.103	0.22	0.0083
500	0.14	0.113	0.17	0.0028

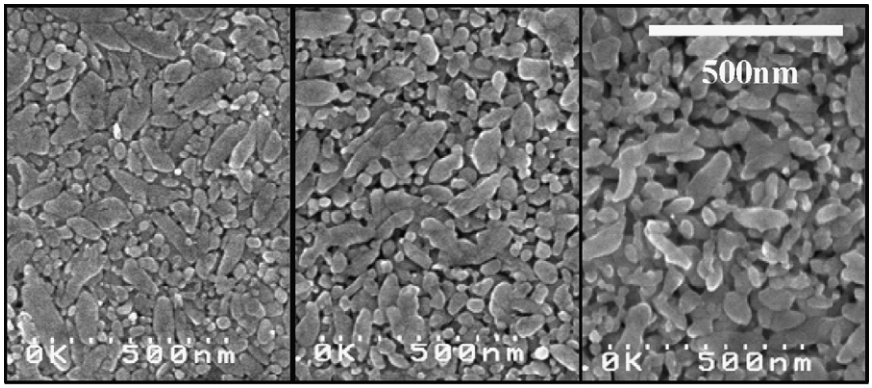

Fig. 6. FE-SEM image of CuO film, annealed at (a) 300 °C, (b) 400 °C and (c) 500 °C.

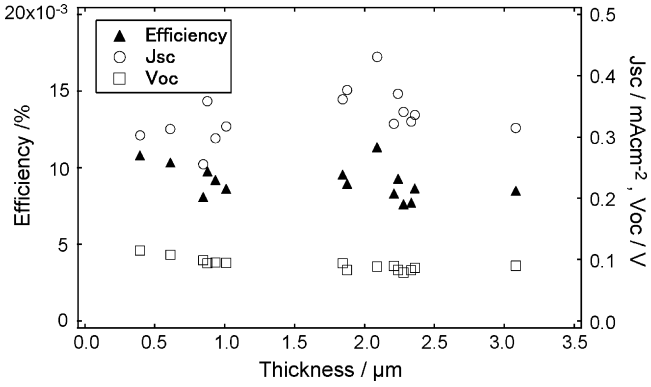

Fig. 7. J_{SC}, V_{OC} and energy conversion efficiency of p-DSCs as a function of CuO electrode thickness.

3.5. Film thickness

Fig. 7 shows J_{SC}, V_{OC}, and the efficiency of p-DSCs of different CuO thicknesses. Adsorbed dye was Fast Green FCF. The current density did not increase much with the thickness. This can be rationalized with the high absorption coefficient of CuO.

4. Conclusions

DSCs constituted of nanoporous p-type semiconductor CuO film dyed with Fast Green FCF and NK-3628, respectively, functioned as p-type dye-sensitized solar cells. The HOMO and LUMO potentials of these dyes are more positive than the valence band and conduction band edges of the semiconductor, respectively, which is favorable for the hole injection to valence band and opposite to the electron injection to the conduction band. Contrarily, CuO electrode sensitized with N3 dye did not generate cathodic current. The LUMO level of N3 is more negative than the conduction band edge, probably resulting in electron injection from the dye to the conduction band and the concomitant recombination of the holes and electrons in the semiconductor. These facts indicated that the widely recognized working principle of n-type DSC is applicable to p-type DSC when inversely interpreted to fit to p-type behavior.

Acknowledgement

This work was supported by the Cooperative Link for Unique Science and Technology for Economy Revitalization (CLUSTER) of Ministry of Education, Culture, Sports, Science and Technology of Japan.

References

[1] B. O'Regan, M. Grätzel, Nature 353 (1991) 737–740.
[2] M. Grätzel, J. Photochem, Photobiol. A: Chem. 164 (2004) 3–14.
[3] J. He, H. Lindström, A. Hagfeldt, S.-E. Lindquist, Sol. Energy Mater. Sol.Cells 62 (2000) 265–273.
[4] J. He, H. Lindström, A. Hagfeldt, S.-E. Lindquist, J. Phys. Chem. B 103 (1999) 8940–8943.
[5] A. Nakasa, H. Usami, S. Sumikura, S. Hasegawa, T. Koyama, E. Suzuki, Chem. Lett. 34 (2005) 500–501.
[6] T. Sakata, K. Hashimoto, M. Hiramoto, J. Phys. Chem. 94 (1990) 3040–3045.
[7] J. Ghijsen, L.H. Tjeng, J. van Elp, H. Eskes, J. Westerink, G.A. Sawatzky, M.T. Czyzyk, Phys. Rev. B 38 (1988) 11322–11330.
[8] A. Hagfeldt, M. Grätzel, Chem. Rev. 95 (1995) 49–68.
[9] A. Hagfeldt, M. Grätzel, Acc. Chem. Res. 33 (2000) 269–277.